

## Reference-Free Calibration for Wearable Core Body Temperature Sensor Based on Single-Heat-Flux Method

Y. Hashimoto , S. Tada, and Y. Nishida 

Department of Mechanical Engineering, Tokyo Institute of Technology, Tokyo 1528552, Japan

Manuscript received 9 April 2024; revised 25 July 2024; accepted 27 July 2024. Date of publication 30 July 2024; date of current version 13 August 2024.

**Abstract**—Core body temperature (CBT) is one of the useful physiological indicators that are linked to physiological changes. Wearable sensors are expected to be developed to monitor CBT easily during activities. A single-heat-flux method is one of the noninvasive techniques that estimate CBT by measuring heat flow changes near the skin with temperature sensors. The method requires calibrating parameters for estimating CBT in advance by comparing them with reference values obtained through another method. The invasive measurement method is generally used to obtain the reference values, which poses a challenge in terms of measurement burden. Here, we propose a new calibration method that does not require acquiring reference values. This method identifies calibration parameters based on the temperature history after the measurement probe is attached. It has been numerically and experimentally confirmed that the estimation accuracy by the method is equivalent to that of a general-purpose electronic thermometer. This outcome decreases the measurement workload in CBT measurement using the single-heat-flux method and significantly enhances its usability.

**Index Terms**—Thermal sensors, core body temperature (CBT), heat flux, reference-free calibration, wearable sensor.

### I. INTRODUCTION

Humans are homeotherms, meaning that they maintain a consistent core body temperature (CBT) to prevent ambient temperature from affecting cellular activity, metabolism, and other necessary physical functions [1]. CBT is also linked to various physiological processes and useful as their indicators, such as circadian rhythms [2], menstrual cycles [3], heat-related illnesses [4], [5], and infectious diseases [6]. For example, heat-related illnesses are conditions that occur when prolonged exposure to a hot and humid environment disrupts the balance of thermoregulatory functions, allowing heat to build up inside the body [7]. To prevent heat-related illnesses, it is recommended to keep the CBT below 38 °C (38.5 °C during heat acclimation) [8], [9]. Therefore, wearable sensors and other technologies to easily monitor CBT during activities are expected to be developed [10]. The CBT measurement conventionally involves invasive procedures, such as the insertion of a temperature sensor inside the body [4], [10]. However, gastrointestinal temperature measurements using ingestible thermometer pills have been successfully applied [11], [12], [13]. Although the period following ingestion of the pills does not affect the validity of the measurements [14], the transit of these pills through the gut and the cost of replacement impose an economic burden during long-duration monitoring. The measurement of gastrointestinal temperature is not always feasible during daily routines or when regular fluid consumption is recommended operational practice [10], [15]. On the other hand, the single-heat-flux method is one of the suitable alternatives during the activity [16]. This method enables the measurement of CBT with a wearable sensor by estimating it from changes in heat flow on the skin surface acquired from a pair of temperature sensors. One of the challenges is the need for initial calibration by comparison with reference values measured by invasive methods. A method using a measurement probe consisting of two pairs of temperature sensors called dual-heat-flux method has been

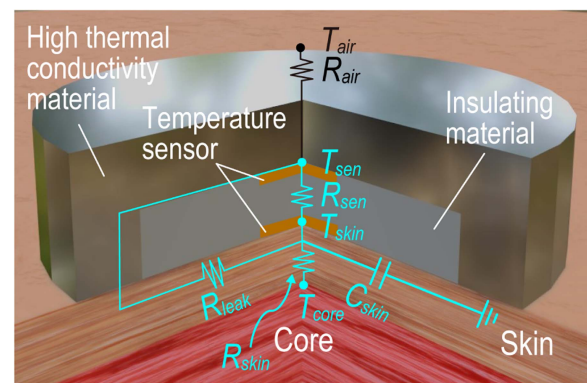


Fig. 1. Overview of a typical CBT measurement by the conventional single-heat-flux method.

reported as a solution to the problem [17]. This method eliminates the need for initial calibration, but its disadvantage is the large size of the measurement probes. Here, we report a new initial calibration method that does not require invasive reference values, as an alternative to the dual-heat-flux method, to address issues with the single-heat-flux method. Specifically, we developed a new method for reference-free initial calibration based on the time history of the temperature sensors immediately after the measurement probe comes into contact with the skin. In addition, we report the validation results of the developed method using test data generated from numerical analysis and human trial.

### II. MATERIALS AND METHODS

#### A. Calibration Theory

Fig. 1 shows an overview of a typical CBT measurement based on the single-heat-flux method [4]. The measurement probe consists of an

Corresponding author: Y. Hashimoto (e-mail: Hashimoto.y.ai@m.titech.ac.jp).  
Associate Editor: Jeong Bong Lee.  
Digital Object Identifier 10.1109/LENS.2024.3435965

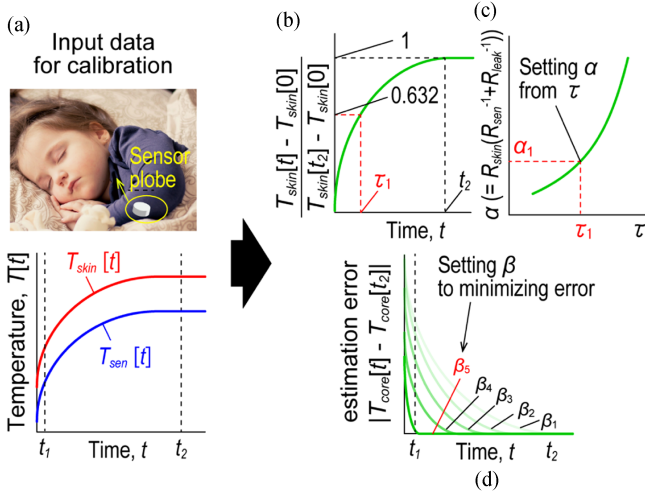


Fig. 2. (a)–(d) Overview of the proposing reference-free initial calibration for the conventional single-heat-flux method.

insulating material, in which two temperature sensors are embedded, and a high thermal conductivity material coated around the insulating material. The CBT ( $T_{core}$ ) is estimated from the skin temperature ( $T_{skin}$ ) and the temperature of the opposite surface ( $T_{sen}$ ) when the probe is in contact with the skin using (1), where  $R_{skin}$ ,  $R_{sen}$ , and  $R_{leak}$  are the thermal resistances of each region and  $C_{skin}$  is the heat capacity of the skin. Conventionally,  $R_{skin}(R_{sen}^{-1} + R_{leak}^{-1})$  and  $R_{skin}C_{skin}$  in (1) must be determined in advance by comparison with reference values measured by other methods [4]

$$T_{core} = T_{skin} + R_{skin} (R_{sen}^{-1} + R_{leak}^{-1}) (T_{skin} - T_{sen}) + R_{skin} C_{skin} \frac{dT_{skin}}{dt}. \quad (1)$$

Fig. 2 provides an overview of the proposed calibration method. The method identifies the calibration parameters based on the time history of temperatures ( $T_{skin}$ ,  $T_{sen}$ ) measured from immediately after probe attachment to the steady state, assuming that the calibration is performed during resting when there are few CBT changes [see Fig. 2(a)]. Specifically, a time constant  $\tau$  is obtained by normalizing the skin temperature at time  $t$  by the initial value and the saturated value at time  $t_2$  [see Fig. 2(b)]. Next,  $\alpha$ , which is one of the calibration parameters shown in (2), is obtained from relationship between  $\alpha$  and  $\tau$ , which is known in advance [see Fig. 2(c)]. Finally, another calibration parameter  $\beta$ , shown in (2), is determined to minimize the evaluation function  $E_{error}$ , shown in (3), describing the time integral of the CBT estimation error from the time  $t_1$  immediately after the start of the measurement to time  $t_2$  when the steady state is reached [see Fig. 2(d)]

$$T_{core} [t] = T_{skin} [t] + \alpha (T_{skin} [t] - T_{sen} [t]) + \beta \frac{dT_{skin} [t]}{dt} \quad (2)$$

$$E_{error} = \int_{t_1}^{t_2} |T_{core} [t] - T_{core} [t_2]| dt. \quad (3)$$

## B. Numerical Simulation Analysis

This section describes the investigation of the proposed method through numerical analysis. To simulate the proposed method, a 2-D axial computational model with two steps was utilized, as shown in Fig. 3. First, a steady-state solution of the temperature distribution

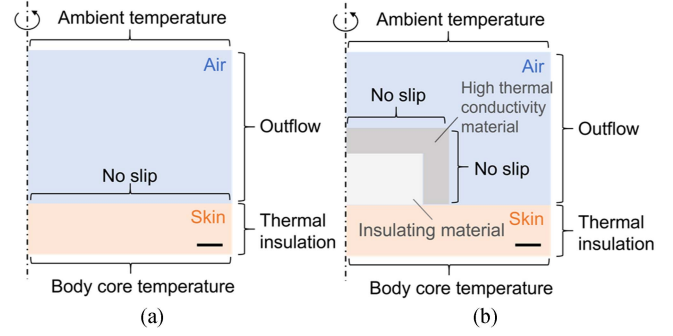


Fig. 3. Two-dimensional axisymmetric computational model and the boundary conditions to compute temperature distributions in the calibration processes. (a) Before attaching the measurement probe. (b) After attaching the measurement probe. Scale bars represent 2.5 mm.

was calculated for the system consisting of skin and air, as shown in Fig. 3(a), where the ambient temperature and CBT were kept constant. The boundary conditions were set, as shown in Fig. 3(a). Subsequently, the time responses of  $T_{skin}$  and  $T_{sen}$  are calculated by utilizing the solution obtained in the previous calculation as the initial value of the temperature distribution. This is achieved by computing the time-dependent solution of the temperature distribution of the system, which comprises the skin, air, and measurement probe, when the measurement probe of the ambient temperature is in contact with the skin, as depicted in Fig. 3(b). The figure illustrates the boundary conditions. The temperature distribution for each part of the measurement system was calculated using the finite-element method to solve (4)–(6), which describe the heat transport between the materials and the airflow [18], [19].

$$\rho C \frac{\partial T}{\partial t} + \rho C \mathbf{u} \cdot \nabla T + \nabla \cdot (-k \nabla T) = 0 \quad (4)$$

$$\rho \left( \frac{\partial \mathbf{u}}{\partial t} + \mathbf{u} \cdot \nabla \mathbf{u} \right) = -\nabla p + \nabla \cdot \left[ \mu \left\{ \nabla \mathbf{u} + (\nabla \mathbf{u})^T \right\} - \frac{2}{3} \mu (\nabla \cdot \mathbf{u}) \right] \quad (5)$$

$$\rho \nabla \cdot \mathbf{u} = 0. \quad (6)$$

The thermal conductivity, heat capacity, density, temperature, velocity (fluid only), viscosity (fluid only), pressure (fluid only), and time of each material are represented by  $k$ ,  $C$ ,  $\rho$ ,  $T$ ,  $\mathbf{u}$ ,  $\mu$ ,  $p$ , and  $t$ , respectively. The matrix  $tr$  is transposed. The measurement probe's geometry and construction materials follow previous studies [4], with polydimethylsiloxane (PDMS) used for insulation and aluminum for high thermal conductivity. COMSOL Multiphysics was used for each calculation.

The relationship between  $\alpha$  and  $\tau$  required for calibration was derived from the temperature distribution of the measurement system when the thermal conductivity, heat capacity, and thickness of skin are varied, using the aforementioned methods. Furthermore, the determination of the calibration parameter  $\beta$  was investigated using the evaluation function  $E_{error}$ .

## C. Prototype

Based on the outcomes of the numerical analysis, the experimental verification of the proposed method using a prototype was conducted. A cylindrical structure (radius of 7.5 mm; thickness of 5.0 mm) with

two thermistors as temperature sensors (LT-2 N-12, Gram Co., Ltd.) embedded in the contact surface with the skin, and the opposite surface was fabricated by molding PDMS as a sensor probe constituting the prototype. UV-curable PDMS (KER-4690—A/B, Shin Etsu Silicone Co., Ltd.), which has less thermal shrinkage and is superior in moldability, was used for PDMS, and the curing conditions during molding were similar to those of previous studies [20], [21]. An aluminum cover structure (thickness of 2.5 mm) was fabricated by machining with an NC milling machine (AE 74, Makino), a machining center (V 33 i, Makino), and a wire-cut electric discharge machine (AD-325 L LN 1 W, Sodick) as the probe cover constituting the prototype.

D. Human Trial

Verification was carried out by applying the prototype to the chest of a healthy subject, while they were resting in a seated position. Medical tape (Micropore Surgical Tape, 3M) was used to attach the prototype. A temperature probe (ITP010-11, Nikkiso-Therm) was inserted through the nasal cavity to measure esophageal temperature as a reference value for CBT [22], [23]. The temperatures inside the prototype ( $T_{skin}$  and  $T_{sen}$ ) were measured immediately after the subject was attached with the prototype in a steady state at room temperature. From the time response of  $T_{skin}$ , the time response curve of  $T_{skin}$  normalized by the initial temperature and the steady state temperature is derived, and the time constant  $\tau$  of the curve is derived. From the relationship between  $\tau$  and  $\alpha$  obtained in the previous section,  $\alpha$  in the measurement system is derived. Substituting  $T_{skin}$ ,  $T_{sen}$ , and the derived  $\alpha$  into (3),  $\beta$  with minimum error is obtained by the generalized reduced gradient method [24].  $t_1 = 180$  s and  $t_2 = 3600$  s were set. The room temperature was set to 20 °C. The experiment was conducted in accordance with the Declaration of Helsinki and approved by the ethics review board of Tokyo Institute of Technology (2023289, 21 December 2023).

III. RESULTS AND DISCUSSION

A. Numerical Simulation Analysis

Fig. 4(a) displays the time variation of normalized skin temperature for different values of  $\alpha$ . It has been confirmed that the temperature response tends to be slower when  $\alpha$  is large, which reflects an effect of either low skin thermal conductivity or large skin thickness. Fig. 4(b) shows the relationship between  $\alpha$  and  $\tau$ , which has been calculated based on the calculation results in Fig. 4(a). A sixth-degree polynomial of  $\tau$  can accurately approximate  $\alpha$ . In addition, the calculation results have been confirmed to be minimally affected by differences in ambient temperature or CBT settings, reflecting the high tolerance of the measurement probes to disturbances [4]. Fig. 4(c) displays the time variation of  $|T_{core}[t] - T_{core}[t_2]|$  when  $\alpha$  is set to 1.30 and  $\beta$  is changed. It has been confirmed that setting an appropriate value of  $\beta$  can reduce the estimation error over a wide time range.

B. Human Trial

Fig. 5(b) displays the measurement results obtained using the prototype [see Fig. 5(a)]. It has been confirmed that each temperature reached a steady state approximately 1 h after the start of measurement. Fig. 5(c) shows the time variation of the normalized skin temperature calculated based on the measurement results. The time constant ( $\tau$ ) of the experimental system is approximately 330.2 s, and the corresponding  $\alpha$  value is identified as 1.377 based on the relationship between  $\tau$  and  $\alpha$  described in Fig. 4(b). This value is as accurate as the one

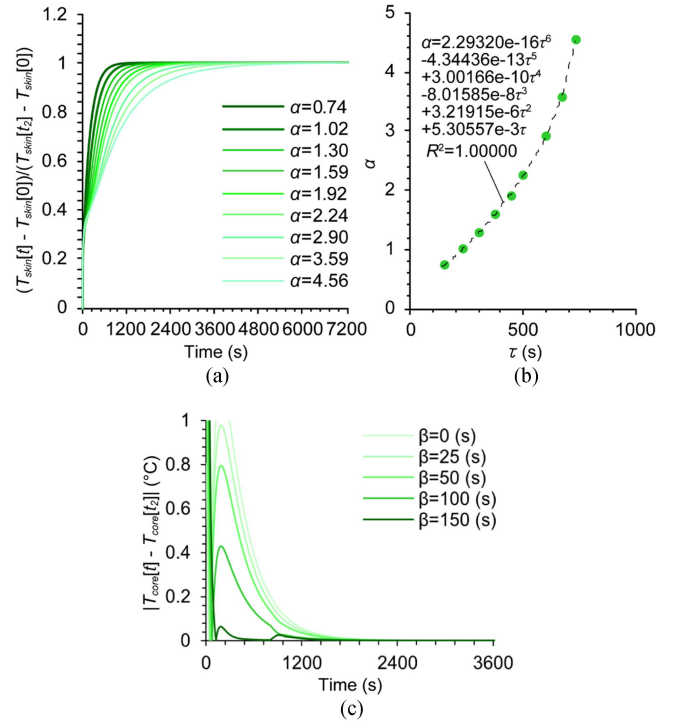


Fig. 4. Overview of the results in the numerical analysis. (a) Time variation of the normalized  $T_{skin}$  for different values of  $\alpha$ . (b) Relationship between  $\tau$  and  $\alpha$  based on the analysis results in (a). (c) Relationship between  $\beta$  and the estimation error for a specific case where  $\alpha = 1.30$ .

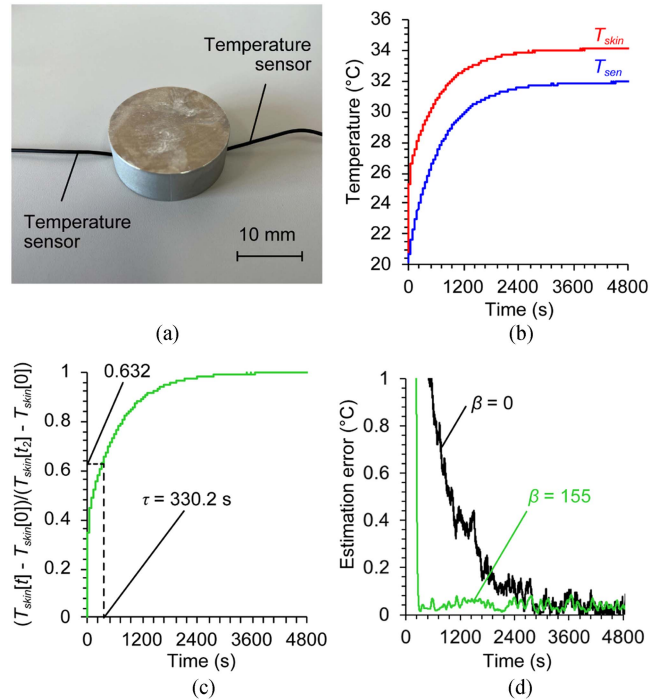


Fig. 5. Overview of the results in the human trial. (a) Prototype. (b) Time variation of  $T_{skin}$  and  $T_{sen}$ . (c) Time variation of the normalized  $T_{skin}$ . (d) Time variation of the absolute value of the estimation error.

estimated from actual measurements (1.367). Fig. 5(d) displays the time variation of the error between the estimated and measured values. Setting  $\beta$  to 155 s, it has been confirmed that  $T_{\text{core}}$  could be estimated with an error lower than 0.1 °C over a wide range of the measurement times starting from 240 s after the measurement began, compared to when no appropriate  $\beta$  was set. This level of accuracy is reasonable when compared to that of electronic thermometers.

### C. Limitation of the Project

The calibration method proposed in this study assumes that measurements are taken while at rest, when there are minimal changes in airflow, air temperature, and CBT. Note that in cases where these changes are significant, such as after exercise or entering/exiting a room with large temperature fluctuations, it is difficult to obtain an accurate time-series curve of skin temperature changes required for calibration. This can affect the acquisition of calibration parameters.

## IV. CONCLUSION

This letter presents a novel method for the initial calibration of a wearable CBT sensor based on the single-heat-flux method without requiring any reference measurement. A numerical analysis and human trial were conducted to demonstrate the proposed method as a proof of concept. The results indicate a satisfactory level of accuracy, with a difference of only 0.1 °C compared to the reference value. The developed method is expected to contribute to enhance the usability of wearable CBT sensors based on the single-heat-flux method. In the future, we will improve the feasibility verification of the development method by increasing the number of subjects. In addition, we will advance the development of wearable health care and medical devices that contribute to the safety and security of people by integrating them with wearable heart rate and sweat sensors [25], [26], [27].

## ACKNOWLEDGMENT

This work was supported in part by the Japan Society for the Promotion of Science Grants-in-Aid for Scientific Research under Grant JP23K19094 and in part by Japan Keirin Autrace Foundation.

This work involved human subjects or animals in its research. Approval of all ethical and experimental procedures and protocols was granted by Human Subject Research Ethics Review Committee of Tokyo Institute of Technology under Application No. 2023289, and performed in line with the Declaration of Helsinki.

## REFERENCES

- [1] J. Kuht and A. D. Farmery, "Body temperature and its regulation," *Anaesth. Intensive Care Med.*, vol. 15, no. 6, pp. 273–278, 2014.
- [2] S. Kimura, Y. Takaoka, M. Toyoura, S. Kohira, and M. Ohta, "Core body temperature changes in school-age children with circadian rhythm sleep—Wake disorder," *Sleep Med.*, vol. 87, pp. 97–104, 2021.
- [3] F. C. Baker, F. Sibozza, and A. Fuller, "Temperature regulation in women: Effects of the menstrual cycle," *Temperature*, vol. 7, no. 3, pp. 226–262, 2020.
- [4] Y. Hashimoto, S. Tada, and Y. Nishida, "Improvement of environment robustness in non-invasive core body temperature sensor studied numerically and experimentally," *Sens. Actuators: A Phys.*, vol. 369, 2024, Art. no. 115136.
- [5] A. Hirata et al., "Body core temperature estimation using new compartment model with vital data from wearable devices," *IEEE Access*, vol. 9, pp. 124452–124462, 2021.
- [6] W. Wang et al., "Real-time personal fever alert monitoring by wearable detector based on thermoresponsive hydrogel," *ACS Appl. Polym. Mater. J.*, vol. 3, pp. 1747–1755, 2021.
- [7] A. Bouchama and J. P. Konochel, "Heat stroke," *New England J. Med.*, vol. 346, no. 25, pp. 1989–1988, 2002.
- [8] D. T. Lamarche et al., "The recommended threshold limit values for heat exposure fail to maintain body core temperature within safe limits in older working adults," *J. Occupat. Environ. Hyg.*, vol. 14, pp. 703–711, 2017.
- [9] G. P. Kenny, S. R. Notley, A. D. Flouris, and A. Grundstein, "Climate change and heat exposure: Impact on health in occupational and general populations," in *Exertional Heat Illness*, W. Adams and J. Jardine, Eds. Cham, Switzerland: Springer, 2019.
- [10] K. Tokizawa, T. Shimuta, and H. Tsuchimoto, "Validity of a wearable core temperature estimation system in heat using patch-type sensors on the chest," *J. Thermal Biol.*, vol. 108, 2022, Art. no. 103294.
- [11] K. Levels, J. J. de Koning, C. Foster, and H. A. M. Daanen, "The effect of skin temperature on performance during a 7.5-km cycling time trial," *Eur. J. Appl. Physiol.*, vol. 112, no. 9, pp. 3387–3395, 2012.
- [12] Y. Hosokawa, W. M. Adams, R. L. Stearns, and D. J. Casa, "Comparison of gastrointestinal and rectal temperatures during recovery after a warm-weather road race," *J. Athletic Training*, vol. 51, no. 5, pp. 382–388, 2016.
- [13] H. A. M. Daanen, V. Kohlen, and L. P. J. Teunissen, "Heat flux systems for body core temperature assessment during exercise," *J. Thermal Biol.*, vol. 112, 2023, Art. no. 103480.
- [14] S. R. Notley, R. D. Meade, and G. P. Kenny, "Time following ingestion does not influence the validity of telemetry pill measurements of core temperature during exercise-heat stress: The journal temperature toolbox," *Temperature*, vol. 8, no. 1, pp. 12–20, 2021.
- [15] D. M. Wilkinson, J. M. Carter, V. L. Richmond, S. D. Blacker, and M. P. Rayson, "The effect of cool water ingestion on gastrointestinal pill temperature," *Med. Sci. Sports Exercise*, vol. 40, pp. 523–528, 2008.
- [16] H.-C. Gunga, M. Sandsund, R. E. Reinertsen, F. Sattler, and J. Koch, "A non-invasive device to continuously determine heat strain in humans," *J. Thermal Biol.*, vol. 33, pp. 297–307, 2008.
- [17] K.-I. Kitamura, X. Zhu, W. Chen, and T. Nemoto, "Development of a new method for the noninvasive measurement of deep body temperature without a heater," *Med. Eng. Phys.*, vol. 32, pp. 1–6, 2010.
- [18] S. Morville et al., "2D axial-symmetric model for fluid flow and heat transfer in the melting and resolidification of a vertical cylinder," in *Proc. COMSOL Conf.*, 2010, pp. 17–19.
- [19] M. B. Turgay and A. G. Yazıcıoğlu, "Numerical simulation of fluid flow and heat transfer in a trapezoidal microchannel with COMSOL multiphysics: A case study," *Numer. Heat Transfer, A*, vol. 73, pp. 332–346, 2018.
- [20] Y. Hashimoto, S. Matsuzawa, and T. Yamamoto, "Subsurface investigation of the surface modification of polydimethylsiloxane by 172-nm vacuum ultraviolet irradiation using ToF-SIMS and VUV spectrometry," *Surf. Interface Anal.*, vol. 50, pp. 752–756, 2018.
- [21] K. Mogi, K. Sakata, Y. Hashimoto, and T. Yamamoto, "A novel fabrication technique for liquid-tight microchannels by combination of a paraffin polymer and a photocurable silicone elastomer," *Materials*, vol. 9, no. 8, 2016, Art. no. 621.
- [22] K. Tsuzuki, K. O. Mizuno, and K. Mizuno, "Effects of humid heat exposure on sleep, thermoregulation, melatonin, and microclimate," *J. Thermal Biol.*, vol. 29, no. 1, pp. 32–36, 2004.
- [23] D. Sumi, K. Okazaki, and K. Goto, "Gastrointestinal function following endurance exercise under different environmental temperatures," *Eur. J. Appl. Physiol.*, vol. 124, pp. 1601–1608, 2024.
- [24] L. S. Lasdon, A. D. Waren, A. Jain, and M. Ratner, "Design and testing of a generalized reduced gradient code for nonlinear programming," *ACM Trans. Math. Softw.*, vol. 4, no. 1, pp. 34–50, 1978.
- [25] Y. Hashimoto, "Lightweight and high accurate RR interval compensation for signals from wearable ECG sensors," *IEEE Sens. Lett.*, vol. 8, no. 6, Jun. 2024, Art. no. 7003304.
- [26] Y. Hashimoto, R. Sato, K. Takagahara, T. Ishihara, K. Watanabe, and H. Togo, "Validation of wearable device consisting of a smart shirt with built-in bioelectrodes and a wireless transmitter for heart rate monitoring in light to moderate physical work," *Sensors*, vol. 22, no. 23, 2022, Art. no. 9241.
- [27] Y. Hashimoto, "Measurement compensation method for wearable microfluidic sweat sensors toward monitoring a wide range of local sweat rates and electrolyte concentration," *IEEE Sens. Lett.*, vol. 7, no. 12, Dec. 2023, Art. no. 4503504.